



BERKELEY LAB

# Overview of STAR Measurements on Correlations and Fluctuations



Yu Hu (胡 昱)\*

for the STAR collaboration



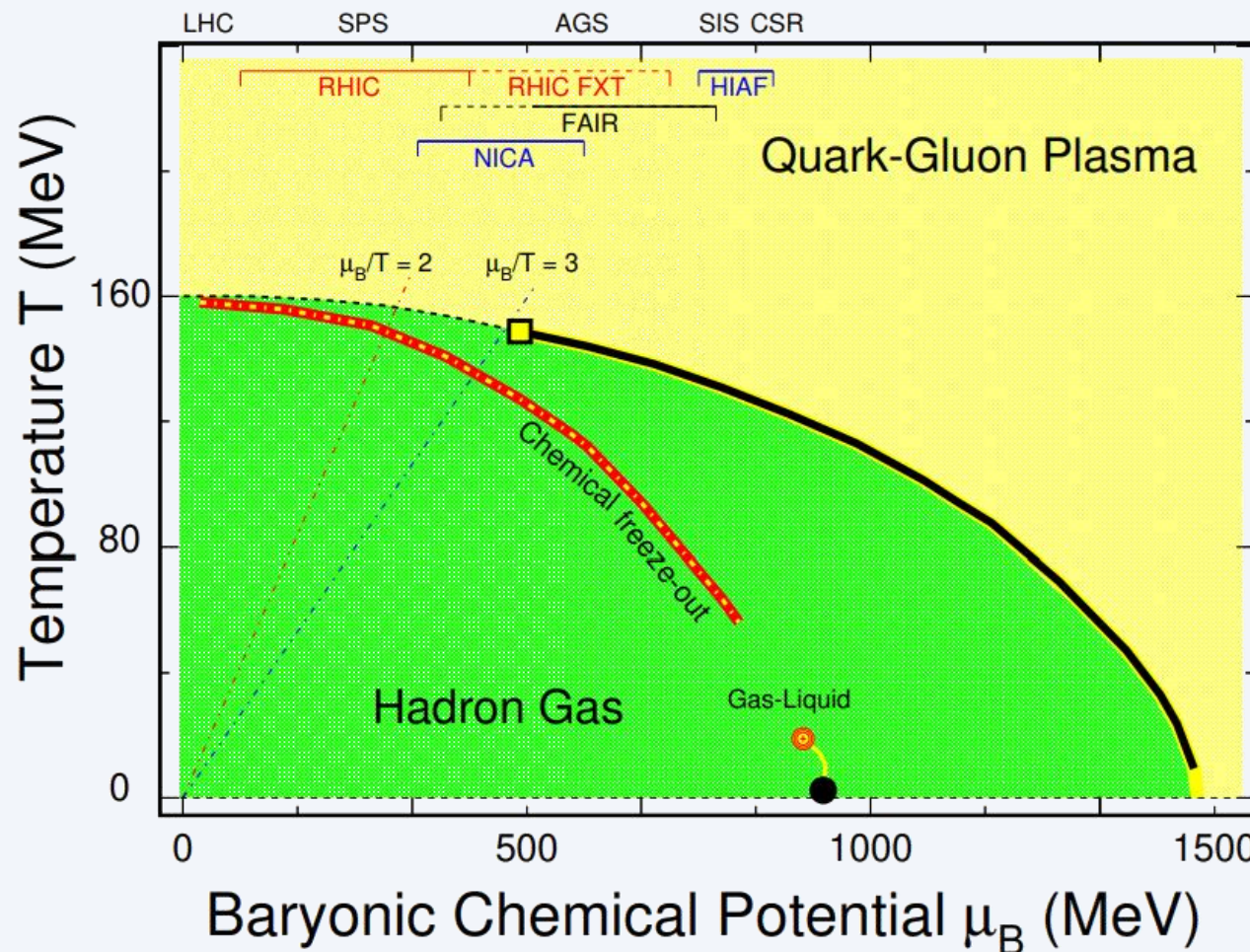
Supported in part by



Office of  
Science

2024.08.28

# QCD Phase Diagram



B. Mohanty and N. Xu, in *Criticality in QCD and the Hadron Resonance Gas* (2021) arXiv:2101.09210

## Phase structure:

### 1. QCD Critical End Point

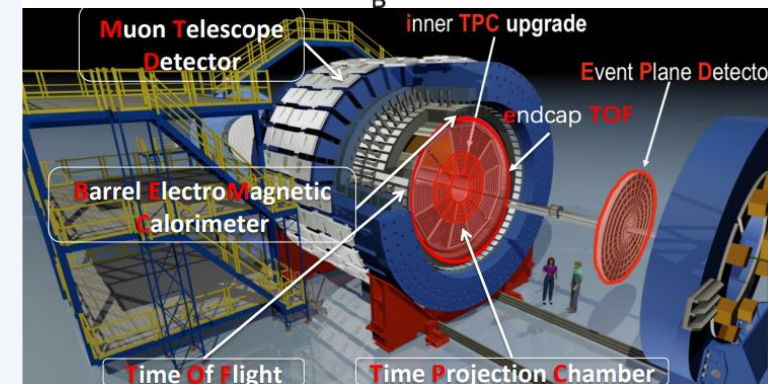
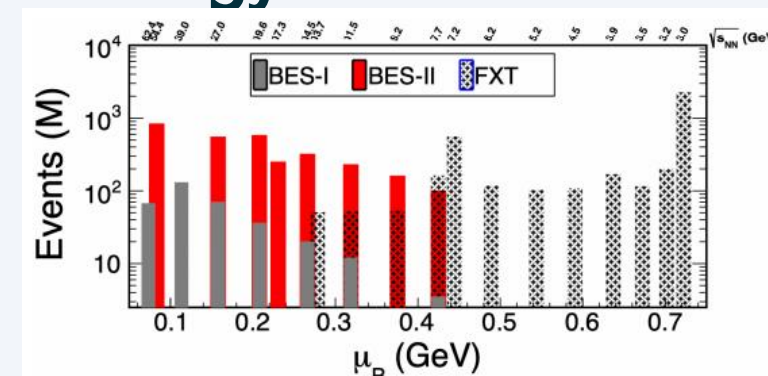
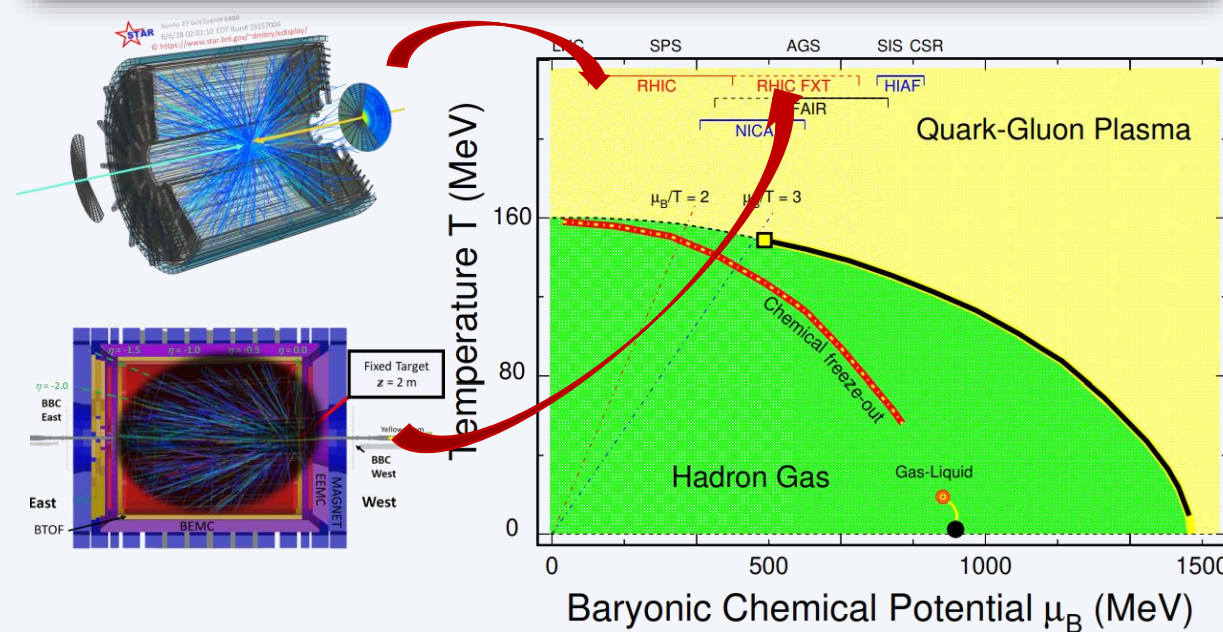
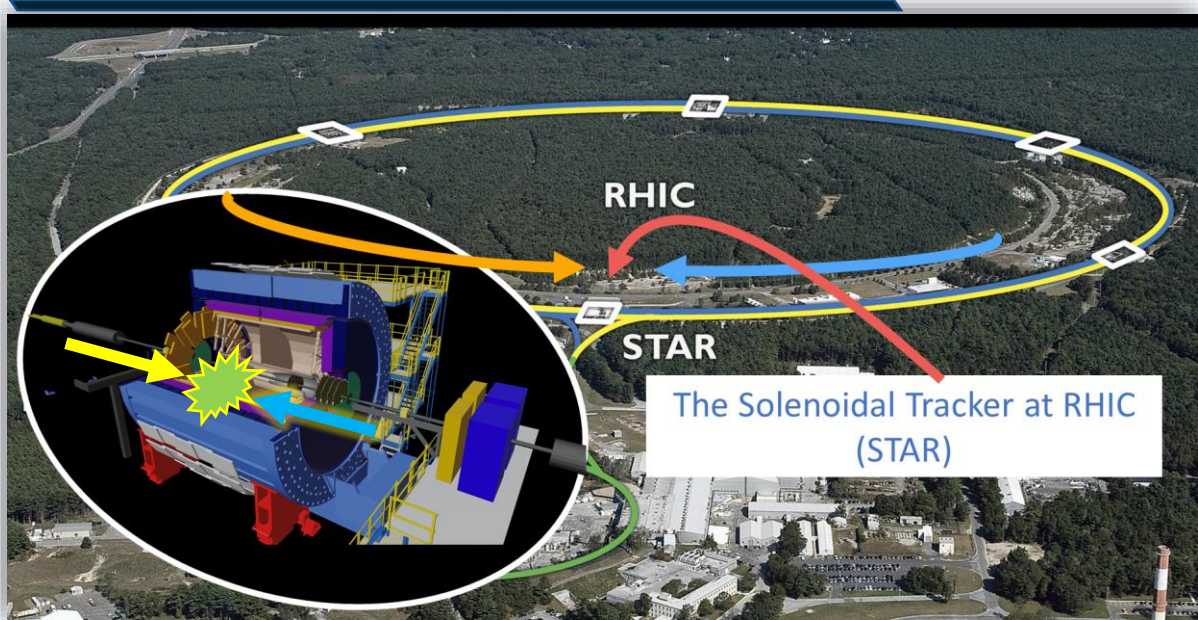
- ❖ Crossover at small  $\mu_B$  ( $\frac{\mu_B}{T} < 3$ ) Lattice
- ❖ **1<sup>st</sup> order P.T. at large  $\mu_B$**  ?
- ❖ **Critical end point**
- ❖ **Recent prediction  $\mu_B \sim 500 - 700$  MeV**

### 2. Equation of State and interaction at high $\mu_B$

- ❖ Structure of nuclear and hyper-nuclei matter
- ❖ Mapping NN, YN, and NNY interactions

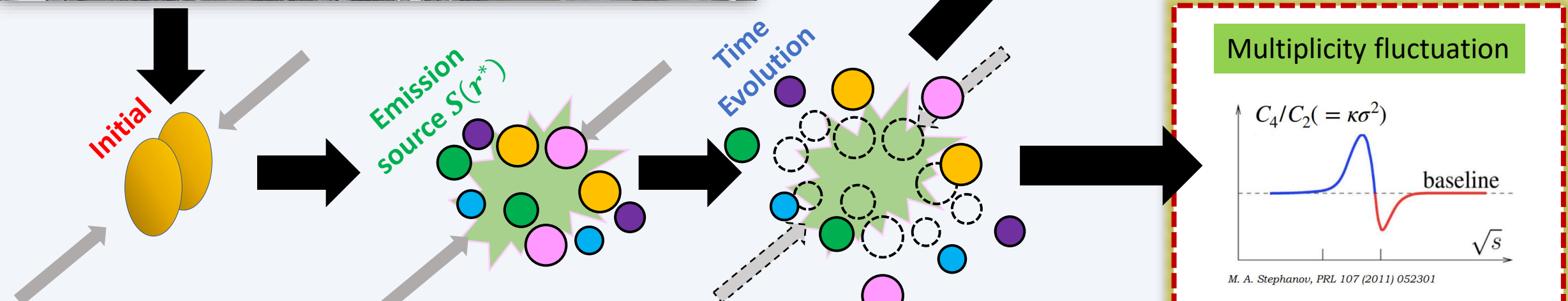
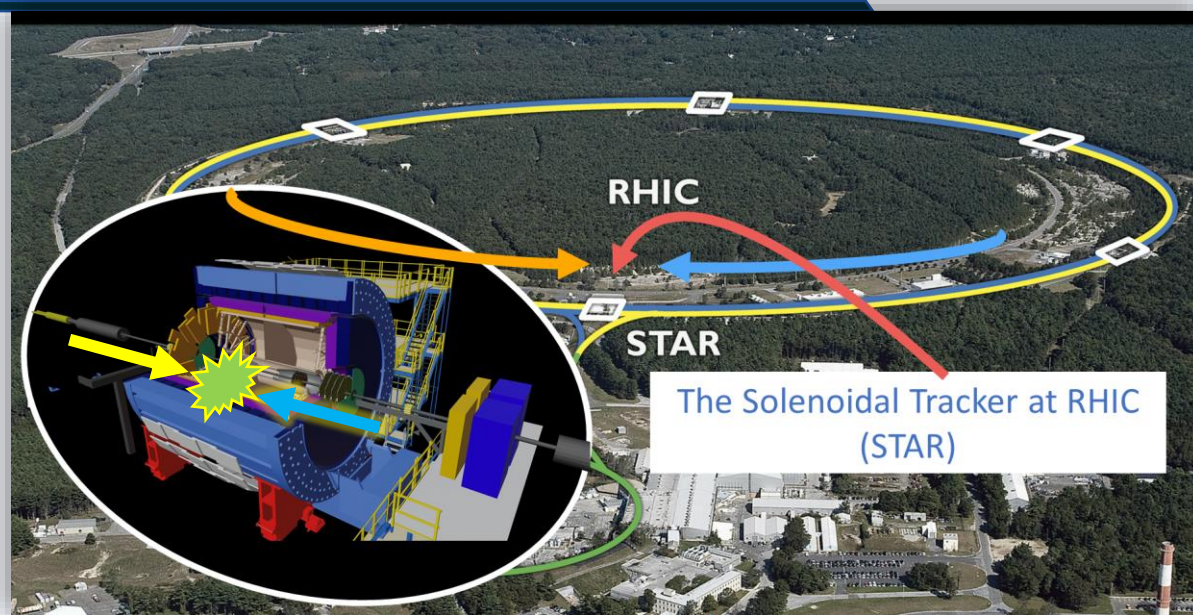
D. A. Clarke, et al. (2024), arXiv:2405.101966

# Heavy Ion Collision Experiment & STAR Beam Energy Scan – II

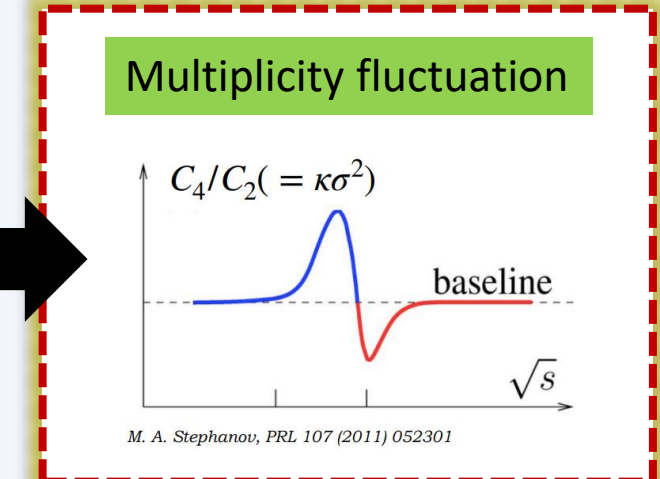
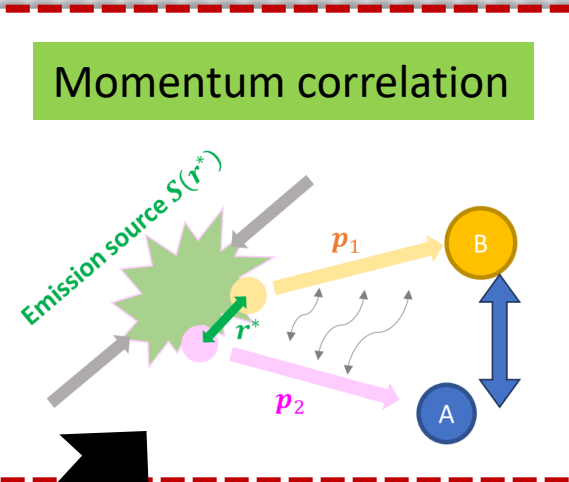


- ❖ Varied collision energies: systematically explore high baryon density region ( $25 < \mu_B < 750$  MeV)
- ❖ Targeted detector upgrades:
  - ❖ iTPC:  $|\eta| < 1$  to  $|\eta| < 1.6$ , lower  $p_T$  reach, improved  $dE/dx$
  - ❖ ETOF: PID at forward rapidity
  - ❖ EPD: Event plane determination & trigger

# Heavy Ion Collision Experiment



❖ Space and time evolution of particle-emitting source + final state interaction



# Net-Proton Distribution

## Cumulants

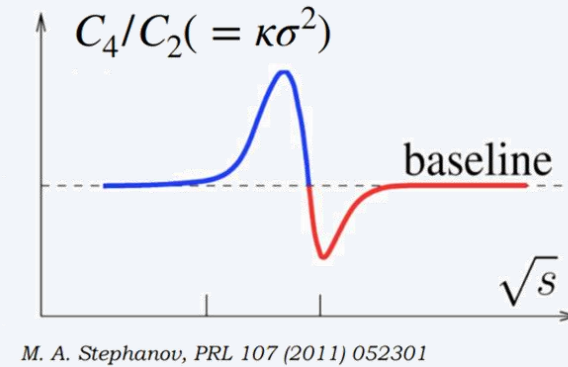
$$\delta n = n - \langle n \rangle$$

$$C_1 = \langle n \rangle$$

$$C_2 = \langle \delta n^2 \rangle$$

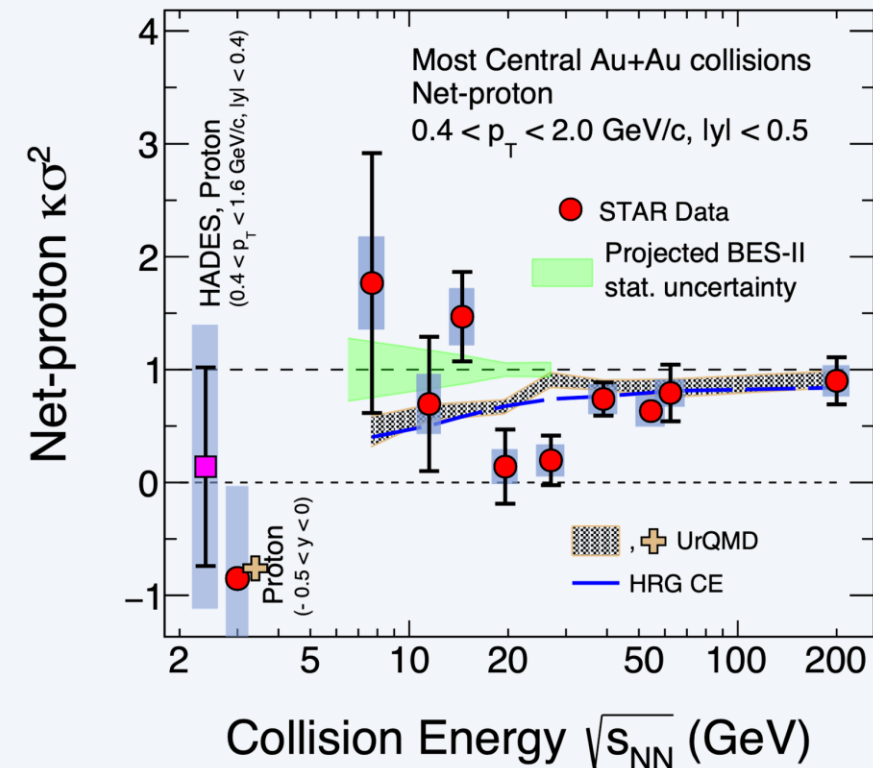
$$C_3 = \langle \delta n^3 \rangle$$

$$C_4 = \langle \delta n^4 \rangle - 3\langle \delta n^2 \rangle$$



Assumption: Thermodynamic equilibrium  
**Non-monotonic  $\sqrt{s_{NN}}$  dependence of  $C_4/C_2$  of conserved quality – Existence of a critical region**

## Measurement @ BES-I



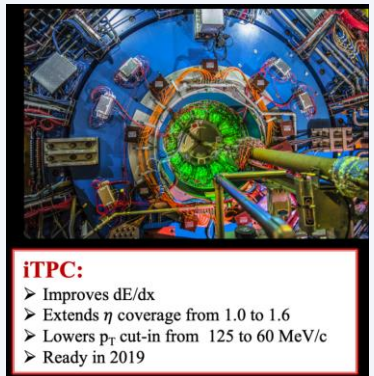
Observed **hint of non-monotonic trend** in BES-I ( $3\sigma$ )  
Robust conclusion require confirmation from precision measurement from BES-II

STAR: PRL 127, 262301 (2021), PRC 104, 24902 (2021)

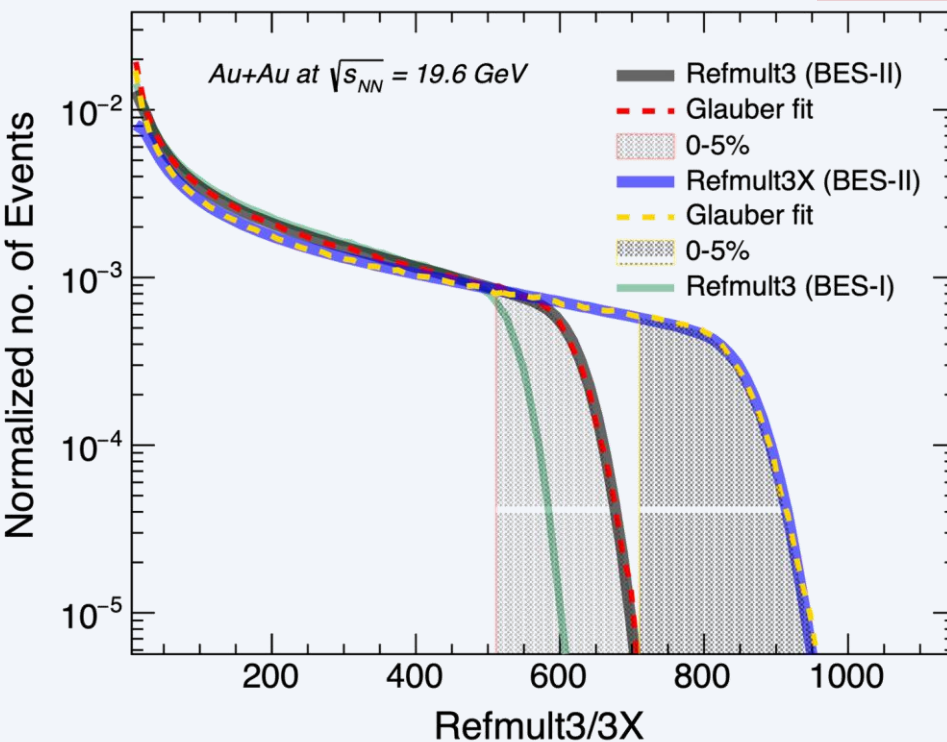
PRL 128, 202302 (2022), PRC 107, 24908 (2023)

HADES: PRC 102, 024914 (2020)

# Precision Measurement of Net-proton Cumulants @ BES-II



$\sqrt{s_{NN}}$ (GeV)	Events BES-I ( $10^6$ )	Events BES-II ( $10^6$ )
7.7	3	<b>45</b>
9.2	-	<b>78</b>
11.5	7	<b>110</b>
14.5	20	<b>178</b>
17.3	-	<b>116</b>
19.6	15	<b>270</b>
27	30	<b>220</b>



- ❖ p and  $\bar{p}$  are excluded to avoid self correlation

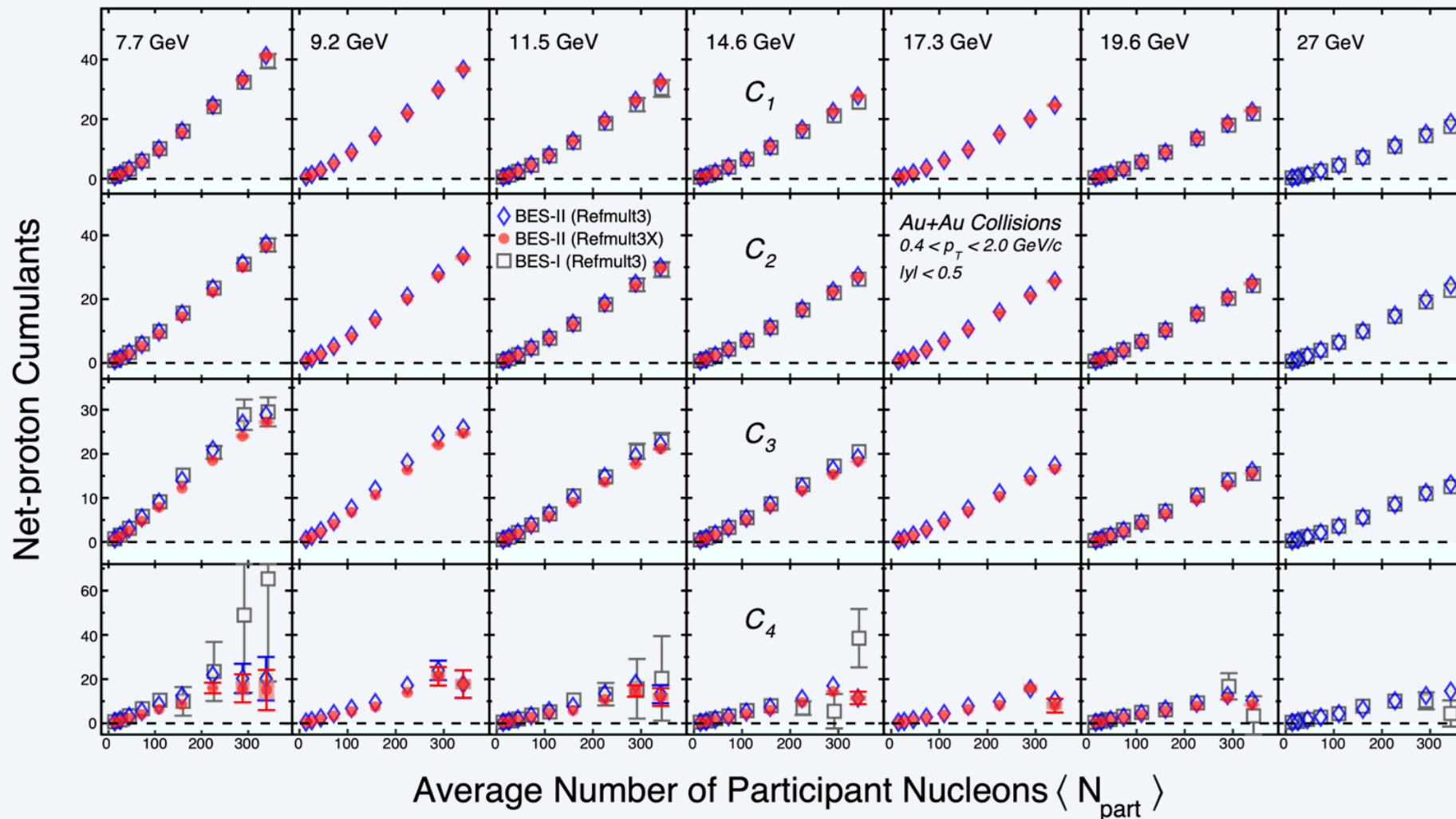
- ❖ Enlarged rapidity acceptance:  
 $|\eta| < 1$  to  $|\eta| < 1.6$
- ❖ Improved particle identification:  
 $p_T \geq 125$  MeV/c to  $p_T \geq 60$  MeV/c
- ❖ Enhanced centrality resolution  
Refmult3 ( $|\eta| < 1$ ) to **Refmult3X ( $|\eta| < 1.6$ )**
- ❖ Better control on uncertainty on efficiency:  
5% to **2%**

## Net-proton cumulants $C_4/C_2$ at 0-5% centrality

7.7 GeV		19.6 GeV	
stat. error	sys. error	stat. error	sys. error
Percentage stat. and sys. error in net-proton cumulants			
61%	29%	22%	11%
Reduction factor in uncertainties, BES-II vs BES-I			
<b>4.7</b>	<b>3.2</b>	<b>4.5</b>	<b>4</b>

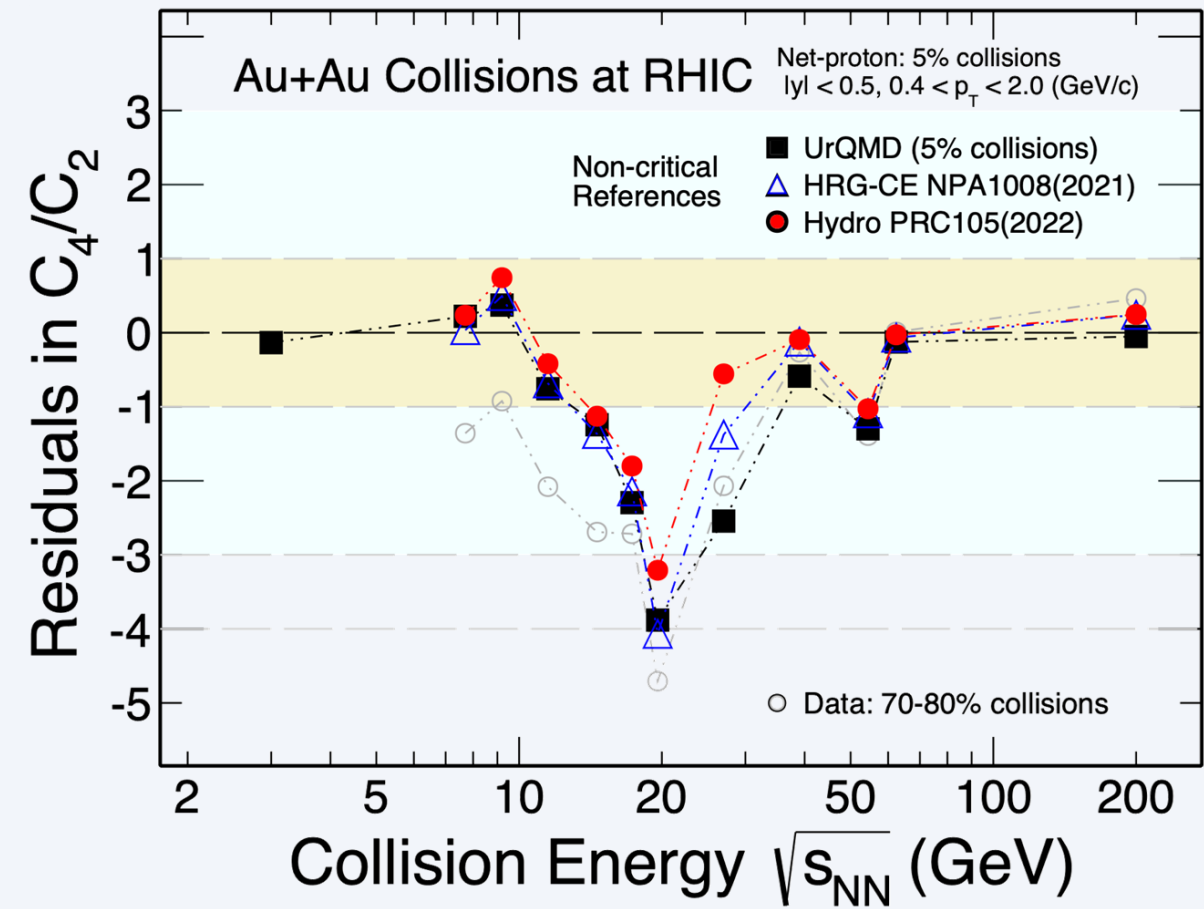
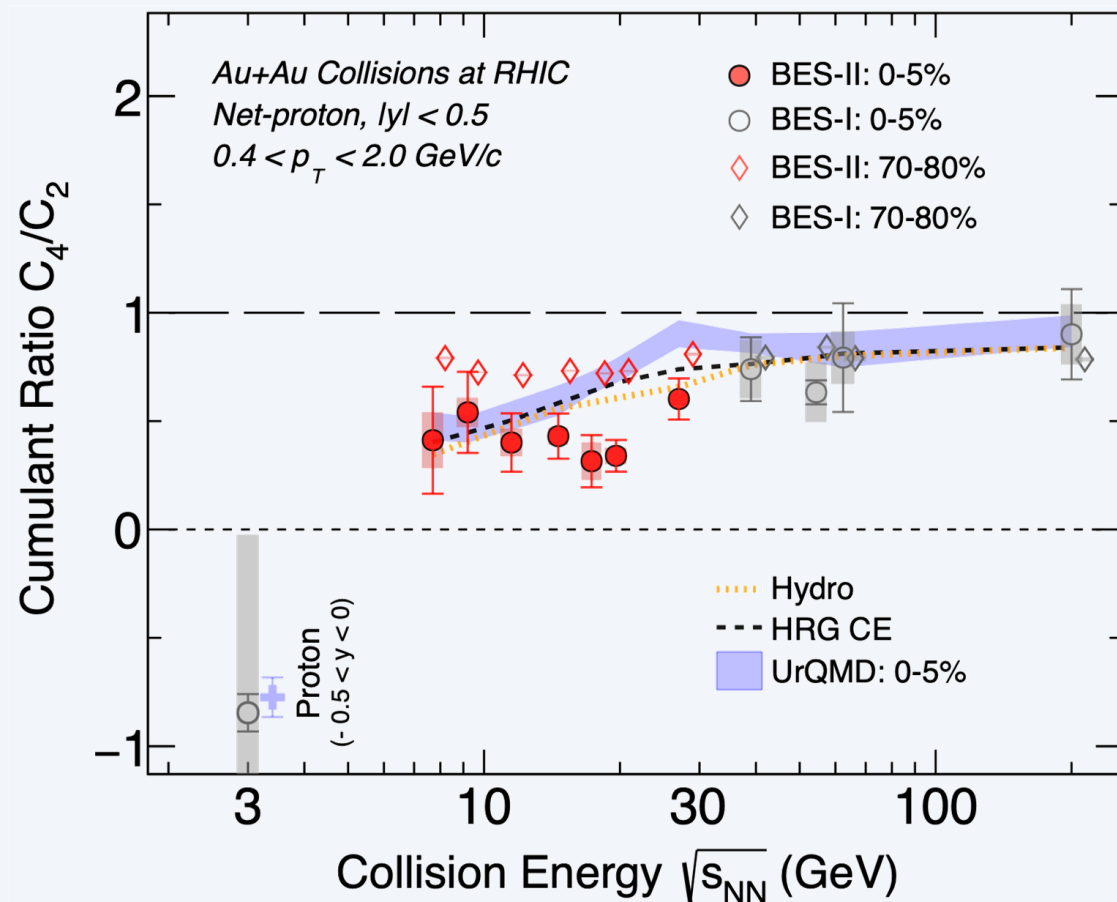
Both **statistical and systematical uncertainties** are significantly reduced in BES-II results

# Precision Measurement of Net-proton Cumulants @ BES-II



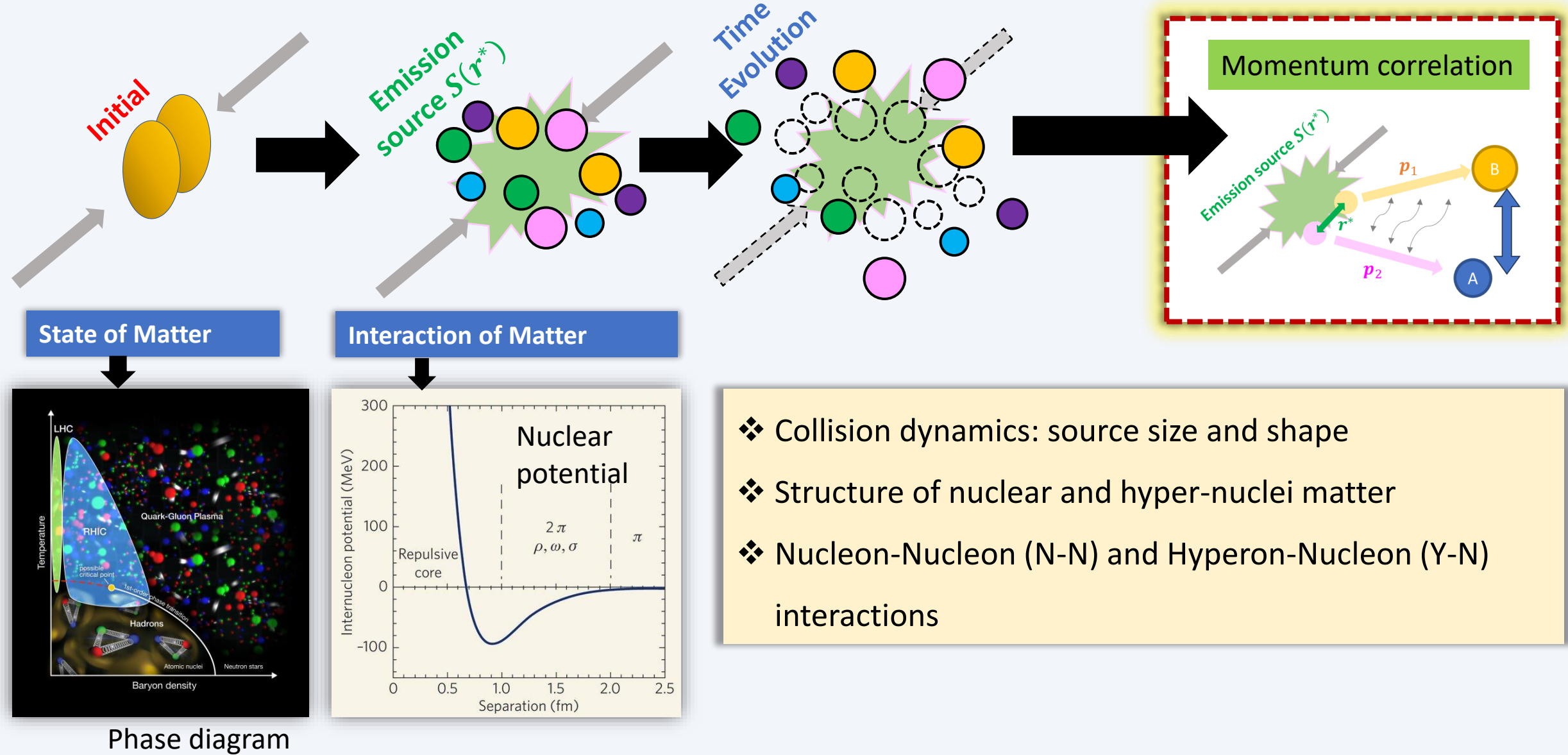
- ❖ The precision measurements from BES-II are consistent with the BES-I results
- ❖ A smooth variation across centrality and collision energy are observed

# CP sensitive observables: $C_4/C_2$



- ❖  $C_4/C_2$  shows minimum around  $\sim 20 \text{ GeV}$  comparing to the non-CP models and 70 - 80% data
- ❖ Maximum deviation: **3.2 - 4.7 $\sigma$**  at  $\sqrt{s_{NN}} \sim 20 \text{ GeV}$  ( $1.3 - 2\sigma$  at BES-I)

# Momentum correlation



<https://www.bnl.gov/newsroom/news.php?a=219079>

<https://www.quora.com/What-does-the-potential-function-for-the-strong-nuclear-force-look-like>

# Correlation Function (CF)

Momentum correlation function:

Statistical

$$C(\mathbf{p}_1, \mathbf{p}_2) \equiv \frac{P(\mathbf{p}_1, \mathbf{p}_2)}{P(\mathbf{p}_1) \cdot P(\mathbf{p}_2)}$$

Single-particle momentum

Modeling

Approximating the emission process and the momenta of the particles:

$$C(\mathbf{k}^*) = \int d^3r^* S(\mathbf{r}^*) |\Psi(\mathbf{r}^*, \mathbf{k}^*)|^2$$

Distribution of the relative distance of particle pair

Relative wave function of the particle pair

Normalization factor

Experimental

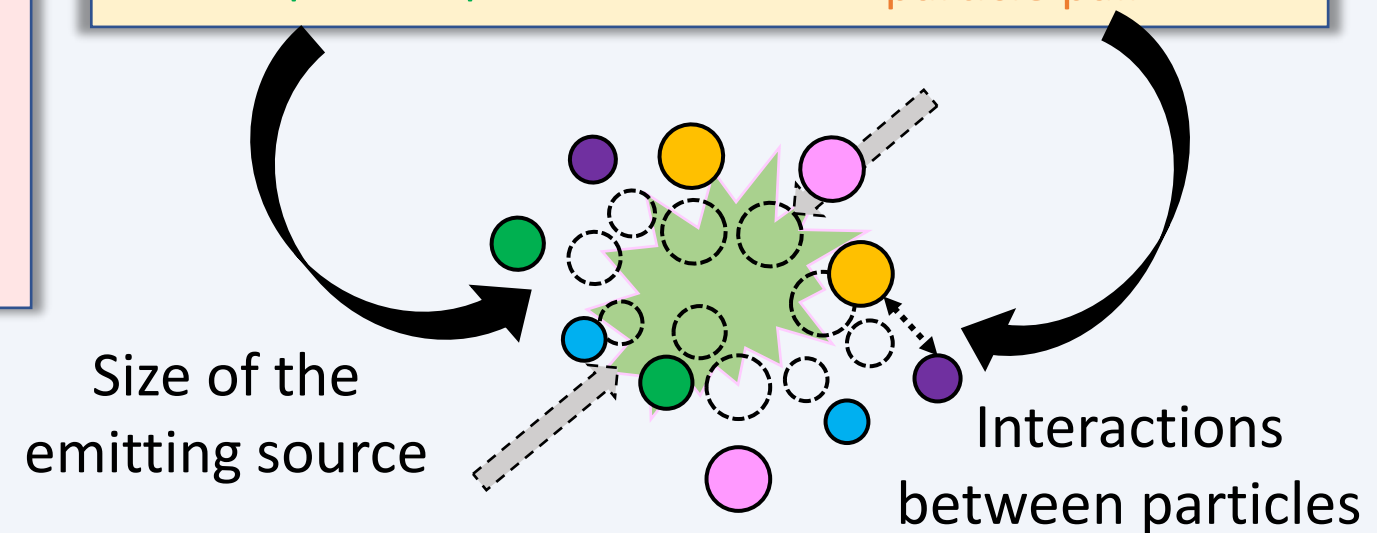
$$C(k^*) = \mathcal{N} \frac{A(k^*)}{B(k^*)}$$

Same events

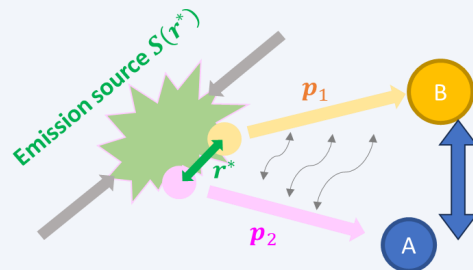
Mixed events

$k^*$ : particle momentum in the pair rest frame

Size of the emitting source



# Kaon Correlation @ High $\mu_B$



- Sinyukov-Bowler<sup>[1]</sup> approach used for  $K^+ - K^+$  and  $\pi^+ - \pi^+$  CF

$$CF(q_{inv}) = N[(1 - \lambda) + K_{coul}(q_{inv}, R_G)\lambda(e^{-R_G^2 q_{inv}^2} + 1)]$$

Coulomb interaction part

QS part

- $N$ : normalize factor;  $\lambda$ : correlation strength

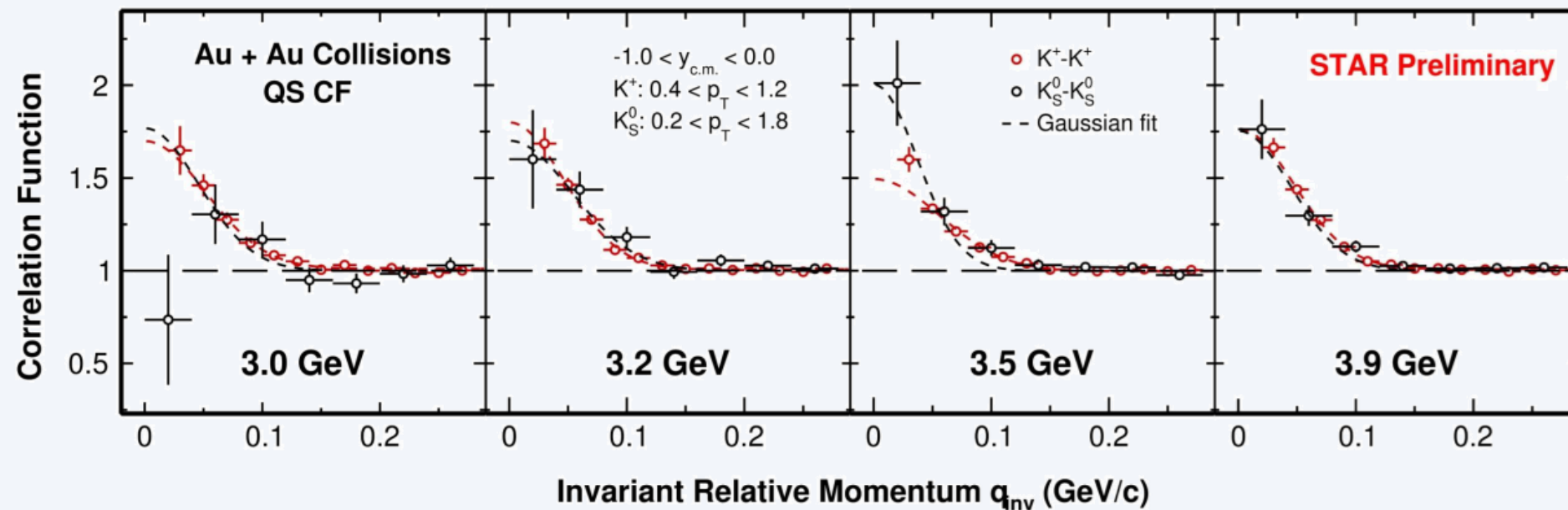
- Lednický-Lyuboshitz (L-L)<sup>[2]</sup> approach used for  $K_S^0 - K_S^0$  CF

$$CF(q) = 1 + \lambda \left( e^{-R_G^2 q_{inv}^2} + \frac{1 - \epsilon^2}{2} \left| \frac{f(k^*)}{r_G} \right|^2 + \frac{4 \operatorname{Re}[f(k^*)]}{\sqrt{\pi} R_G} F_1(q_{inv} R_G) - \frac{2 \operatorname{Im}[f(k^*)]}{R_G} F_2(q_{inv} R_G) \right)$$

Strong interaction part

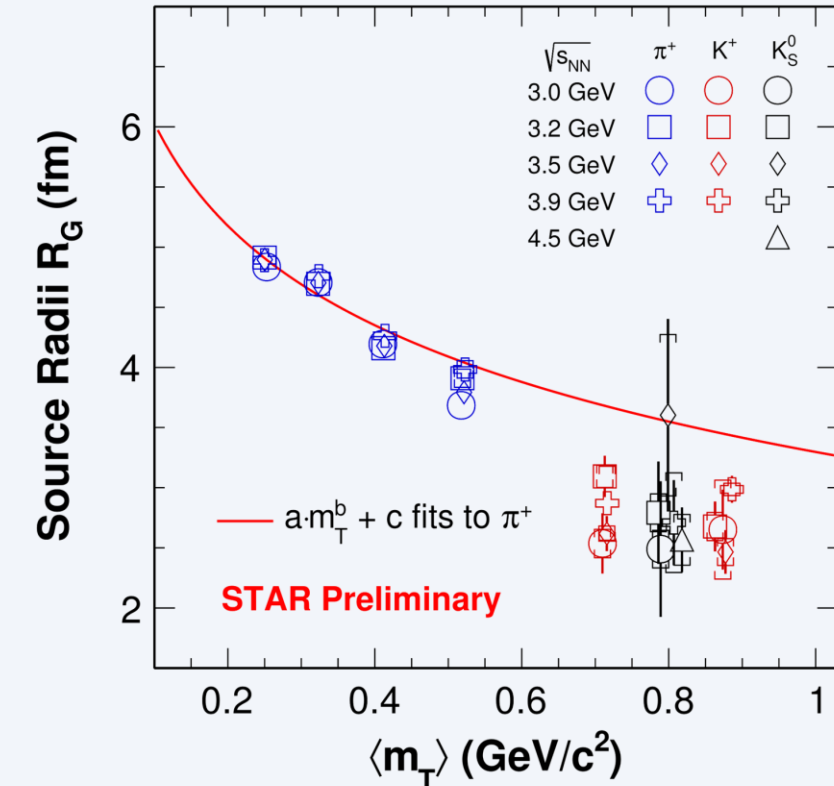
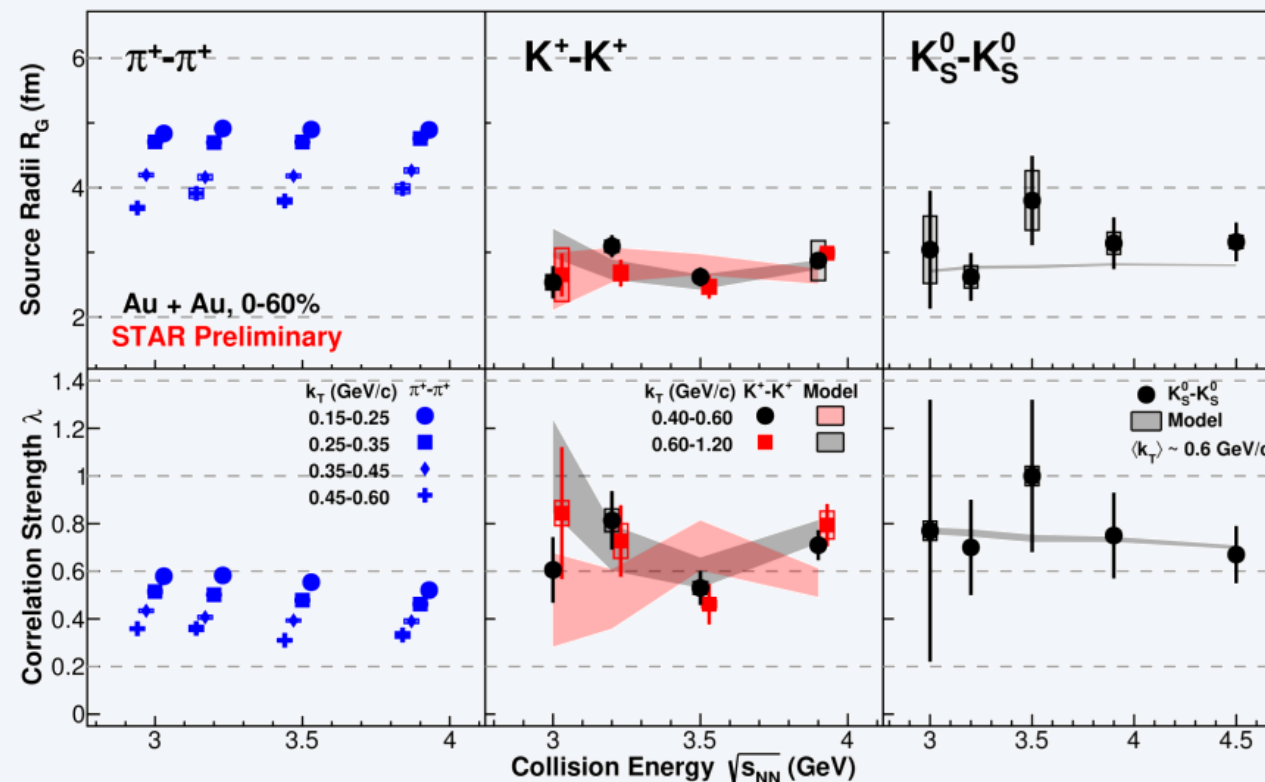
QS part

Kaon abundance asymmetry



- ❖ No significant energy dependence is observed for both  $K^+K^+$  and  $K_S^0K_S^0$
- ❖ CF for  $K^+K^+$  and  $K_S^0K_S^0$  are consistent under current precision

# Pion & Kaon Correlation @ High $\mu_B$

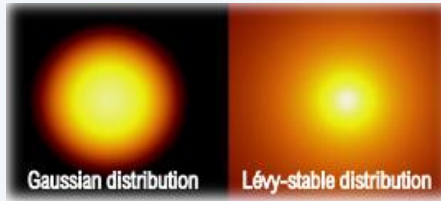


- ❖ Within  $3.0 < \sqrt{s_{NN}} < 3.9$  GeV, no clear energy dependence was observed for both source radii and correlation strength
- ❖  $R_G(\pi) > R_G(K)$
- ❖ Different  $\langle m_T \rangle$  depends for  $\pi$  and  $K$

$$m_T = (k_T^2 + m^2)^{1/2}$$

# Pion Correlation w. Lévy source

$$C = \int d^3r^* S(r^*) |\psi|^2$$



Lévy parametrization without final state effects:

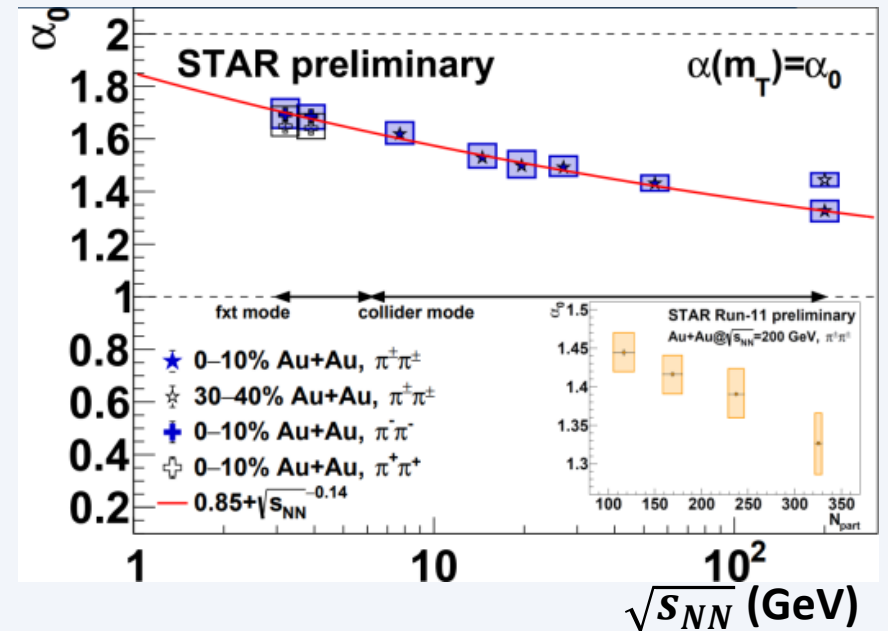
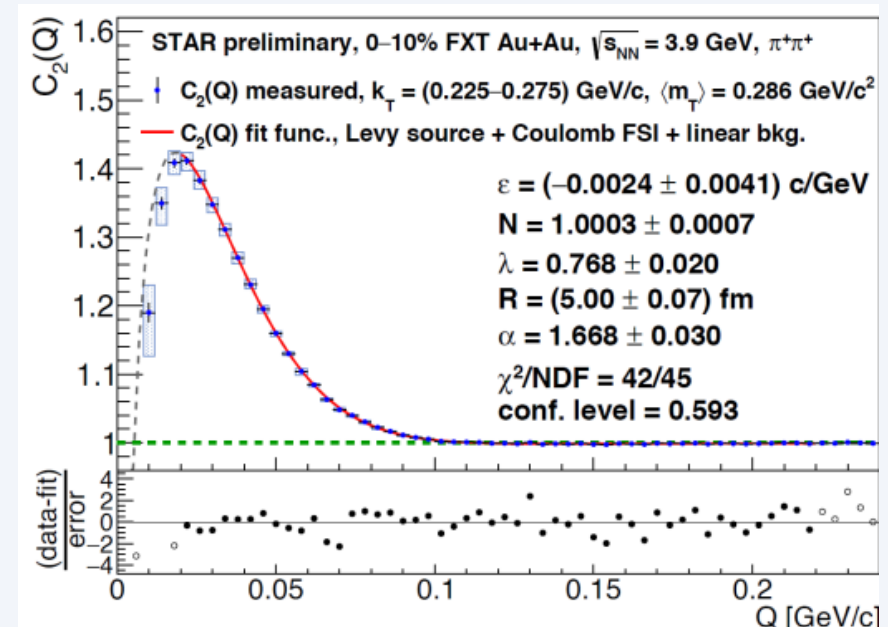
$$C^{(0)}(Q) = 1 + \lambda \cdot e^{-|RQ|^\alpha}$$

$Q$ : LCMS three-momentum difference  $Q = \sqrt{(p_{1x} - p_{2x})^2 + (p_{1y} - p_{2y})^2 + q_{long,LCMS}^2}$

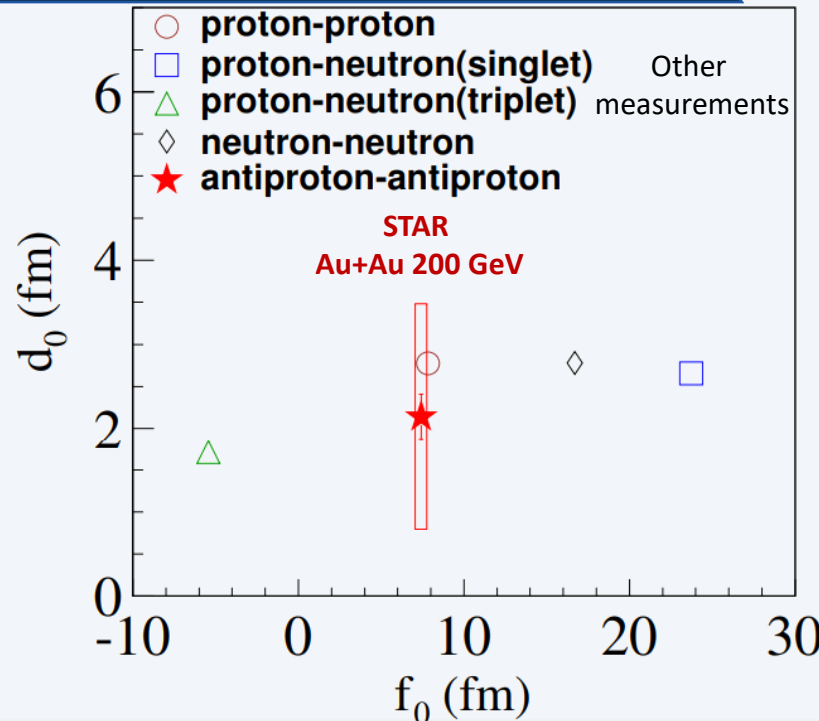
$\lambda$ : correlation strength

$\alpha$ : Lévy exponent

- ❖ Lévy-source + Coulomb FSI have a good description of the CF
- ❖  $\alpha < 2$  indicate a non-gaussian shape of the sources at all collision energies

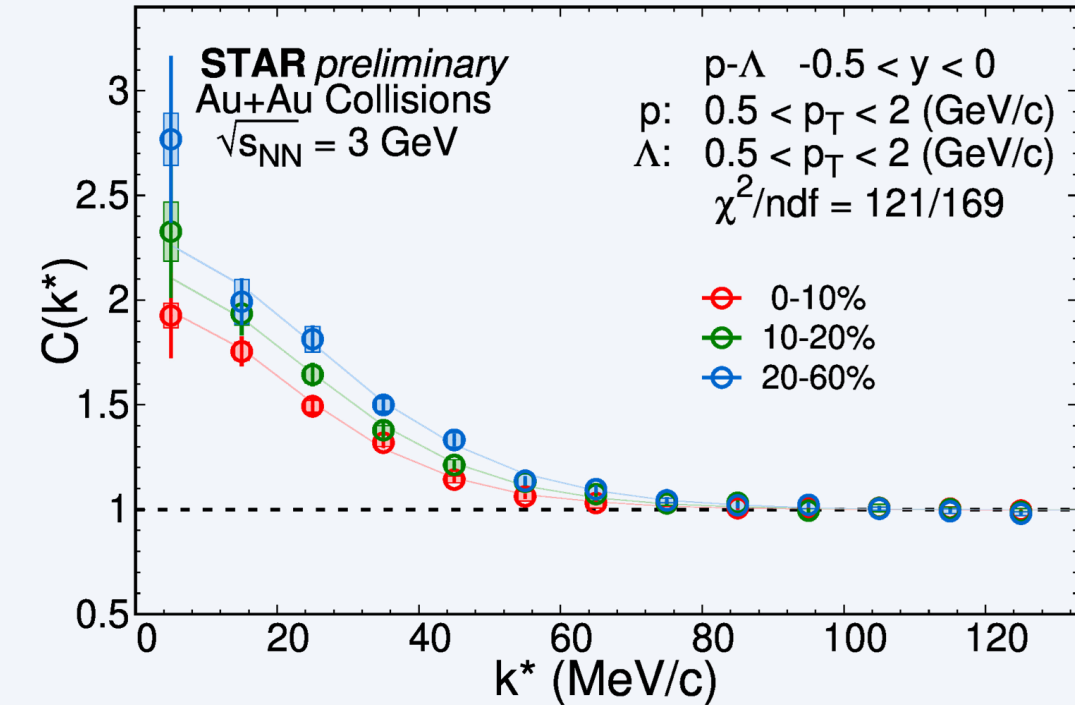


# p-p & p- $\Lambda$ Correlation Functions



Scattering length ( $f_0$ ) for  $p - p$ :

- ❖ Low-E experiment found  $f_0 = 7.806 \pm 0.003$  fm
- ❖ Correlations in HIC with **Lednicky-Lyuboshitz (L-L) approach**:  $f_0 \sim 7$  fm



Correlation functions for  $p - \Lambda$ . With L-L approach:

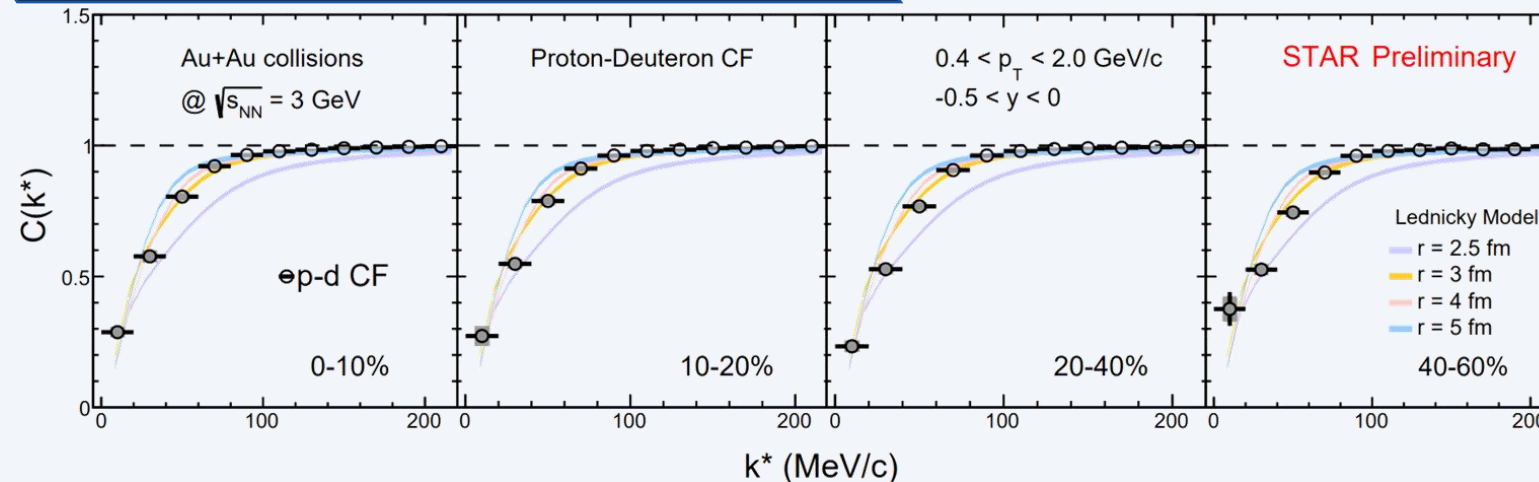
- ❖ Simultaneous fit to data in different centralities/rapidity
- ❖ Spin-avg scattering length ( $f_0$ ) and effective range ( $d_0$ ):

$$f_0 = 2.32^{+0.12}_{-0.11} \text{ fm}$$

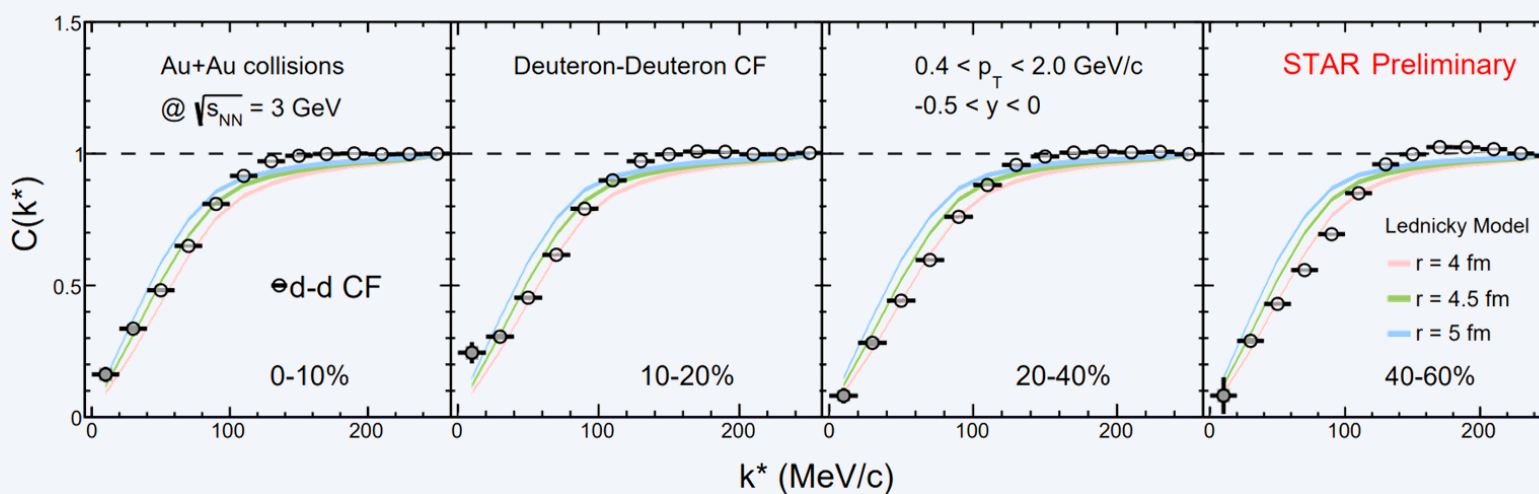
$$d_0 = 3.5^{+2.7}_{-1.3} \text{ fm}$$

- ❖ A valid method to study the interaction between baryons
- ❖ Scattering length is much larger in p-p compare with p- $\Lambda$

# p-d & d-d Correlation Functions



Consistent with L-L model with Coulomb + repulsive interaction



Consistent with L-L model with Coulomb + QS + repulsive interaction

## Model prediction

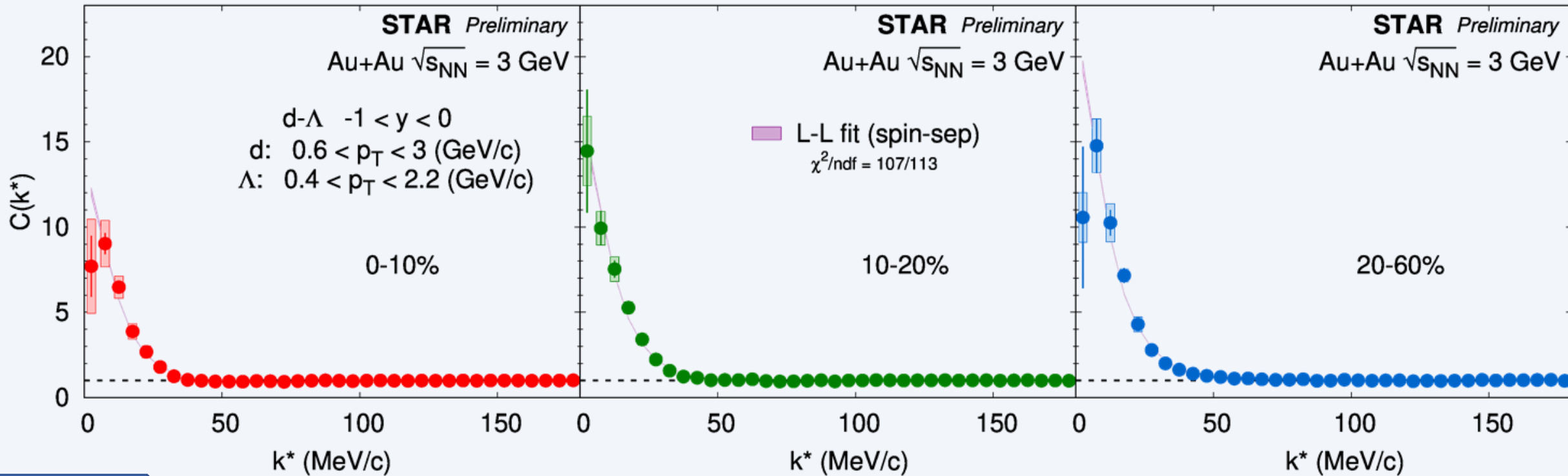
p-d	$f_0$ (fm)	$d_0$ (fm)
Doublet	-2.73	2.27
Quartet	-11.88	2.63
d-d	$f_0$ (fm)	
Singlet	-10.2	
Quintet	-7.5	

❖ Models which only has two-body interactions can well describe our p-d and d-d data

J. Arvieux, NPA 221 (1974) 253

I.N. Filikhin and S.L. Yakovlev, Phys. Atom. Nucl. 63 (2000) 55 / 216  
Robert B. Wiringa, et. al, Phys. Rev. C 51 (1995) 38-51

# d- $\Lambda$ Correlation Functions @ STAR



## Corrections

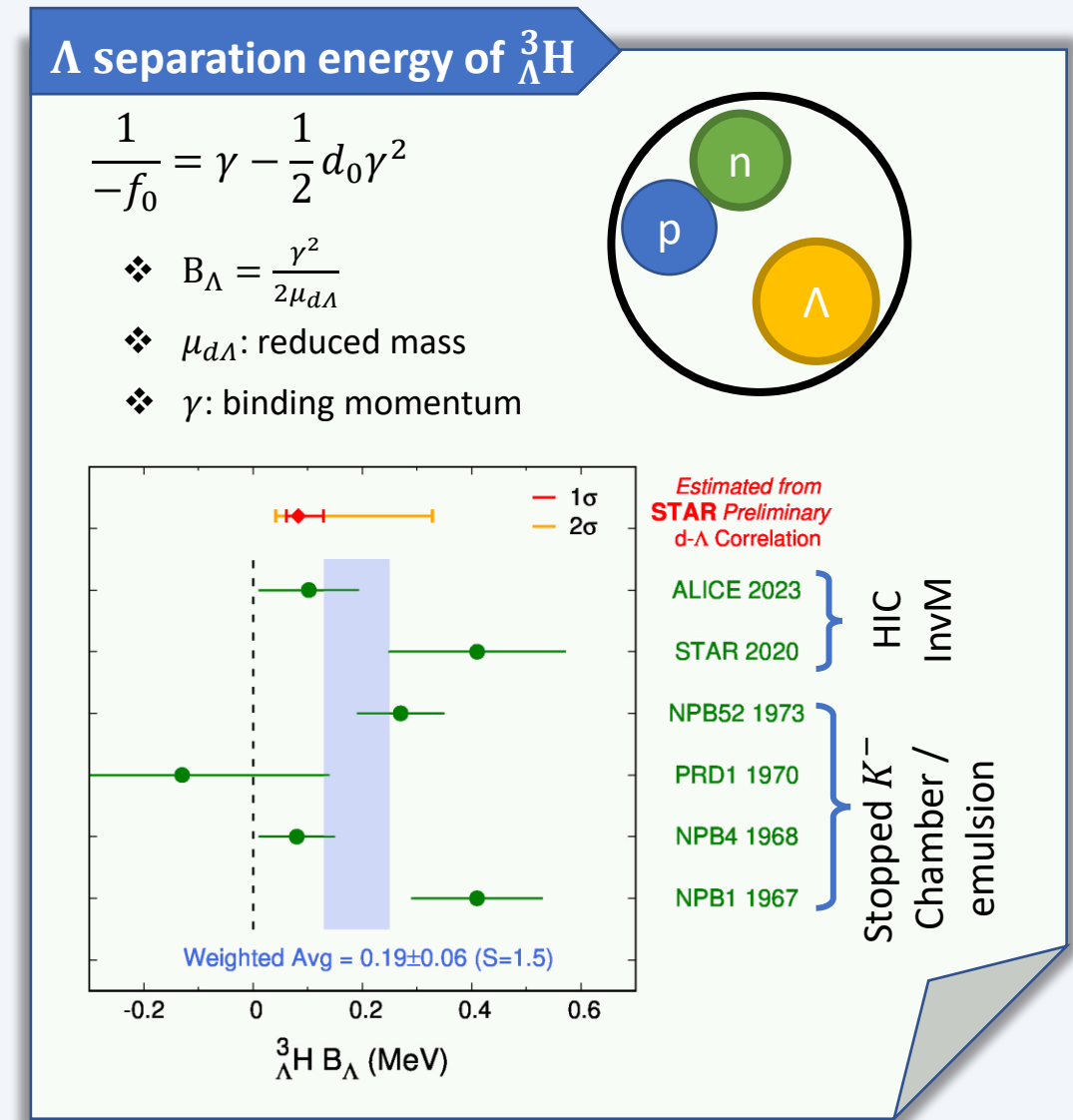
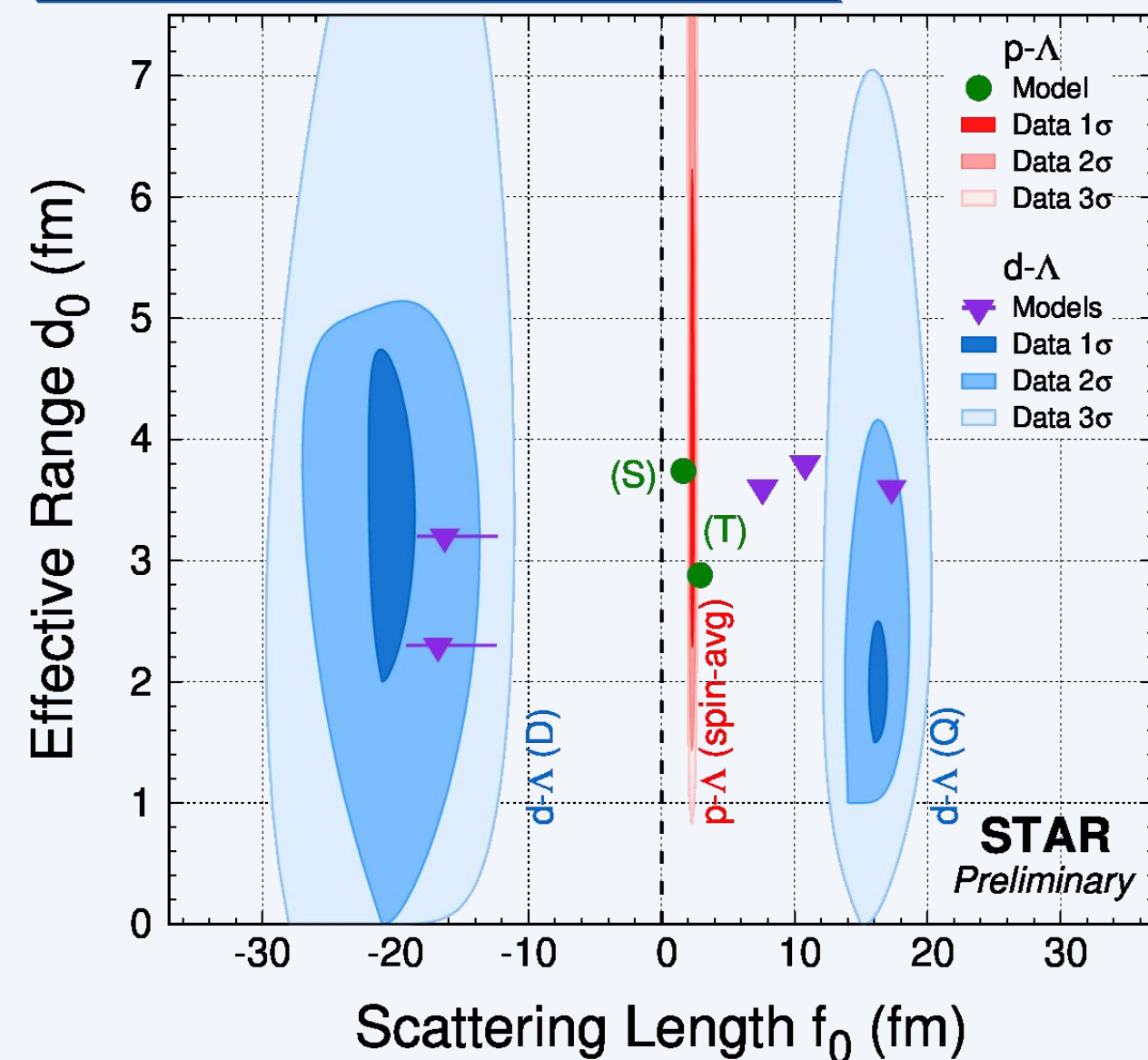
1. Purity correction
2. Track splitting & merging
3. Contamination from  ${}^3\text{H} \rightarrow \pi^- + p + d$  decay

- ❖ First d- $\Lambda$  correlation measurements in the heavy-ion collision experiment
- ❖ Simultaneous fit to data in different centralities
  - ❖  $R_G^i, f_0(D), d_0(D), f_0(Q)$ , and  $d_0(Q)$  with Lednicky-Lyuboshitz approach

$f_0(D) = -20^{+3}_{-3}$ fm	$d_0(D) = 3^{+2}_{-1}$ fm
$f_0(Q) = 16^{+2}_{-1}$ fm	$d_0(Q) = 2^{+1}_{-1}$ fm

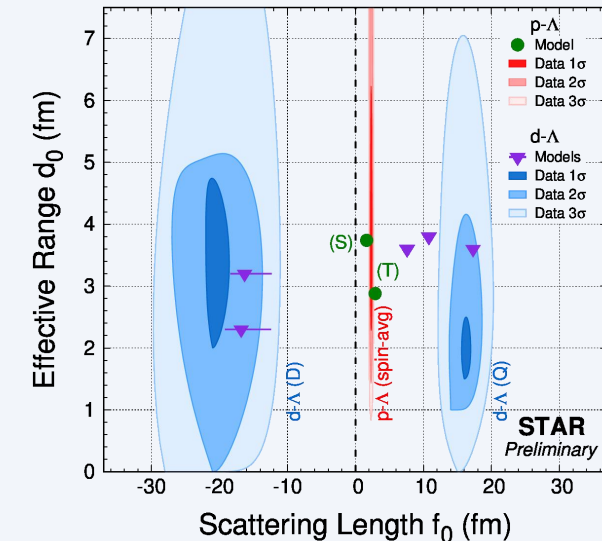
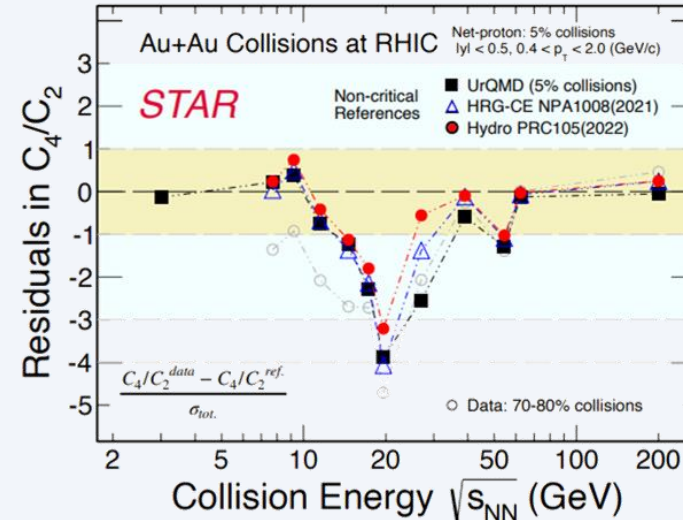
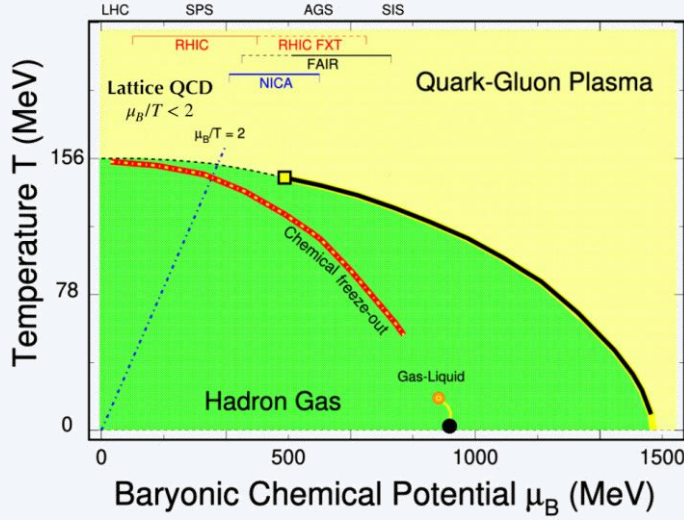
- ❖  $\Lambda$  feed-down correction not applied due to unknown d- $\Sigma/\Xi$  correlation
- ❖ Momentum smearing effect negligible

# Scatterings Length ( $f_0$ ) and Effective Range ( $d_0$ )



- ❖ Constraint fit for d- $\Lambda$ , require  $f_0(D) < 0$
- ❖ Edge of d- $\Lambda$  contours are shown with Bezier smooth to improve the visibility

# Summary



## ❖ QCD Critical End Point

- ❖ Precision measurement of net-proton fluctuations in BES-II significantly reduced the uncertainty
- ❖  $3.2 - 4.7\sigma$  maximum deviation for net-proton  $C_4/C_2$  w.r.t non-CP model/70-80% data is observed
  - **Need more theory input**
- ❖ Stay tuned for the measurements at FXT energies

## ❖ Equation of State

- ❖ A large scope of meson-meson and baryon-baryon correlations is studied at STAR
- ❖ First experimental measurement of d-Λ correlation function
- ❖ FXT program: a unique probe to NN, and YN interactions



# Thank you!



Supported in part by  
U.S. DEPARTMENT OF  
**ENERGY**

2024.08.28

# Higher order Cumulants Measurements at BES-I

## Phase I of BES program (BES-I): Au+Au collisions

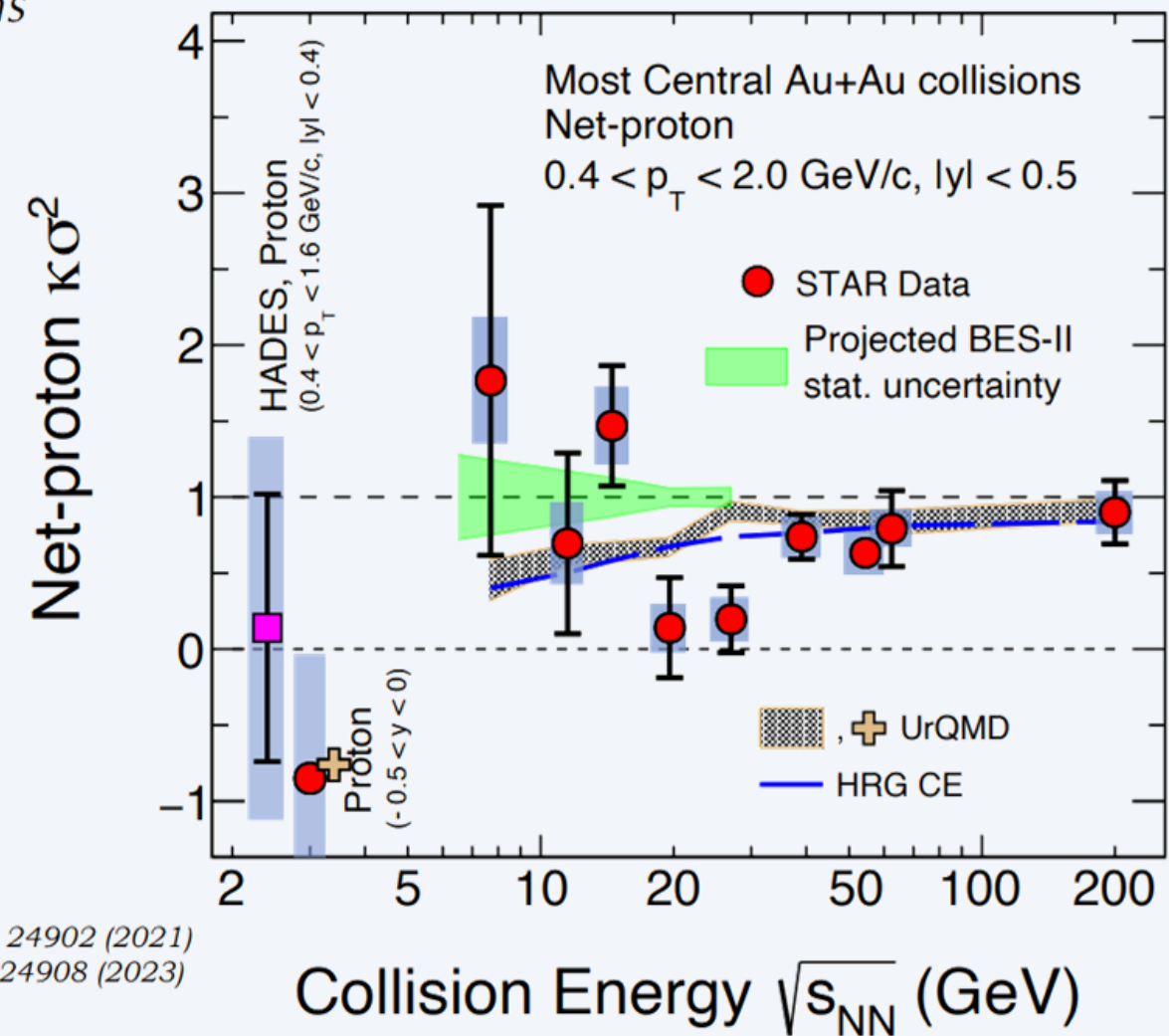
J. Cleymans, et. al, PRC. 73, 034905 (2006)

$\sqrt{s_{NN}}$ (GeV)	Events ( $10^6$ )	$\mu_B$ (MeV)
200	220	25
62.4	43	75
54.4	550	85
39	92	112
27	31	156
19.6	14	206
14.5	14	262
11.5	7	316
7.7	2.2	420
3.0	140	750

STAR : PRL 127, 262301 (2021), PRC 104, 24902 (2021)

: PRL 128, 202302 (2022), PRC 107, 24908 (2023)

HADES: PRC 102, 024914 (2020)



# Low-E scattering experiment & Effective Range Expansion

Low energy elastic scatterings:

$$k \cot(\delta(k)) = -\frac{1}{a} + \frac{1}{2} r_0 k^2 + O(k^4)$$

$a$ : phase shift

$a$ : Fermi scattering length at zero energy

$r_0$ : effective range

$O$ : higher order contribution

Cross section:

$$\lim_{k \rightarrow 0} \sigma_e = 4\pi a^2$$

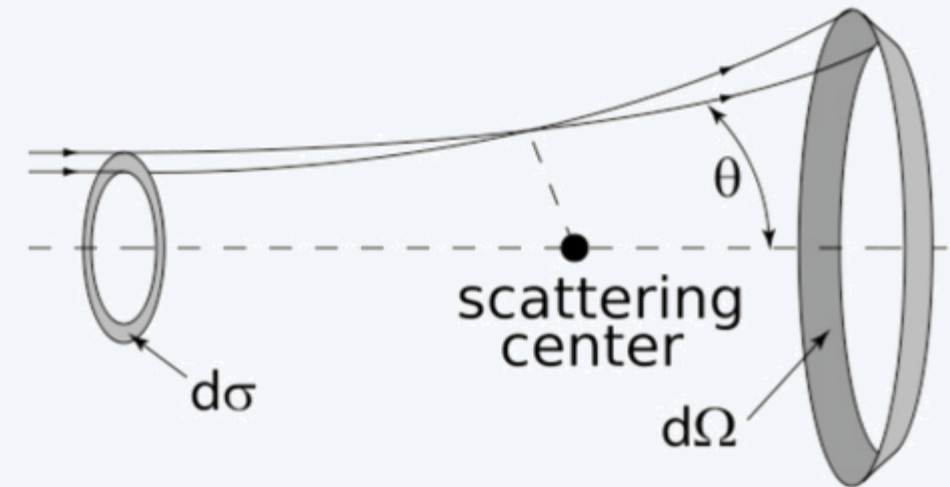
Binding energy:

$$\frac{1}{a} = \gamma - \frac{1}{2} r_0 \gamma^2$$

$$\diamondsuit \quad B = \frac{\gamma^2}{2\mu}$$

$\diamondsuit \quad \mu$ : reduced mass

$\diamondsuit \quad \gamma$ : binding momentum



H. A. Bethe, Phys. Rev. 76 (1949) 38

For the n-p scattering:

$$S_0: \quad a = -23.714 \text{ fm} \quad r_0 = 2.73 \text{ fm}$$

$$S_1: \quad a = 5.425 \text{ fm} \quad r_0 = 1.749 \text{ fm}$$

$$\rightarrow B_d = 2.2 \text{ MeV}$$

# Lednicky-Lyuboshitz (L-L) Approach

R. Lednicky, et al. Sov.J.Nucl.Phys. 35 (1982) 770

J. Haidenbauer, Phys.Rev.C 102 (2020) 3, 034001

L. Fabbietti, et al., Ann.Rev.Nucl.Part.Sci. 71 (2021) 377-402

Michael Annan Lisa, et al., Ann.Rev.Nucl.Part.Sci. 55 (2005) 357-402

Approximating the emission process and the momenta of the particles:

*Modeling*

$$C(\mathbf{k}^*) = \int d^3r^* S(r^*) |\Psi(r^*, \mathbf{k}^*)|^2$$

Distribution of the relative distance of particle pair

Relative wave function of the particle pair

Major Assumptions

Source

❖ Smoothness approximation for source function\*

❖ Static and spherical Gaussian source

- Single particle source:  $S_i(x_i, p_i^*)$

- Pair source (radius  $R_G$ ):  $S(x, p^*) \propto e^{-x^2/2R_G^2} \delta(t - t_0)$

Wave function

❖ S-wave scattering wave

❖ Effective range expansion for  $\Psi(r^*, \mathbf{k}^*)$

❖ Approximate the wave function by its asymptotic form

Gaussian source approximation:

$$S(r^*) = (2\sqrt{\pi}R_G)^{-3} e^{-r^{*2}/4R_G^2}$$

Scattering amplitude:

Consider only S-wave     $\Psi(r^*) = e^{-ir^*\cdot\mathbf{k}^*} + \frac{f(\mathbf{k}^*)}{r^*} e^{ir^*\cdot\mathbf{k}^*}$

$$f(\mathbf{k}^*) \approx \left( \frac{1}{f_0} + \frac{d_0 \mathbf{k}^{*2}}{2} - i\mathbf{k}^* \right)^{-1}$$

Scattering length:

$$a \rightarrow -f_0$$

Effective range:

$$r_0 \rightarrow d_0$$

Lednicky-Lyuboshitz (L-L) approach

$R_G$  : spherical Gaussian source of pairs

$f_0$  : scattering length

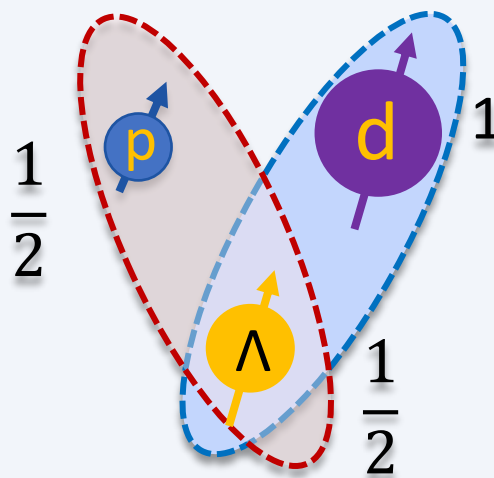
$d_0$  : effective range

\*The smoothness approximation has been checked for expanding thermal sources, found to be very reasonable for large (RHIC-like) sources, but still questionable for smaller sources

# Modeling with Separated Spin States

Modeling

Singlet State	$^1S_0$	(S)
Triplet State	$^3S_1$	(T)



Doublet State	$^2S_{1/2}$	(D)
Quartet State	$^4S_{3/2}$	(Q)

Approximating the emission process and the momenta of the particles:

$$C(\mathbf{k}^*) = \int d^3r^* S(\mathbf{r}^*) |\Psi(\mathbf{r}^*, \mathbf{k}^*)|^2$$

Source      Wave function

Spin averaged

$|\Psi(\mathbf{r}^*, \mathbf{k}^*)|^2$  expanded with averaged parameters:  $\bar{f}_0$  and  $\bar{d}_0$

$$|\Psi(\mathbf{r}^*, \mathbf{k}^*)|^2 \rightarrow \boxed{f_{S1}} |\Psi_{S1}(\mathbf{r}^*, \mathbf{k}^*)|^2 + \boxed{f_{S2}} |\Psi_{S2}(\mathbf{r}^*, \mathbf{k}^*)|^2$$

Spin separated

$$C(\mathbf{k}^*) = \int d^3r^* S(\mathbf{r}^*) \left( \frac{1}{3} |\Psi_{1/2}(\mathbf{r}^*, \mathbf{k}^*)|^2 + \frac{2}{3} |\Psi_{3/2}(\mathbf{r}^*, \mathbf{k}^*)|^2 \right)$$

For separated spin states in d-Lambda

$$\boxed{f_0(D)}$$

$$\boxed{d_0(D)}$$

$$\boxed{f_0(Q)}$$

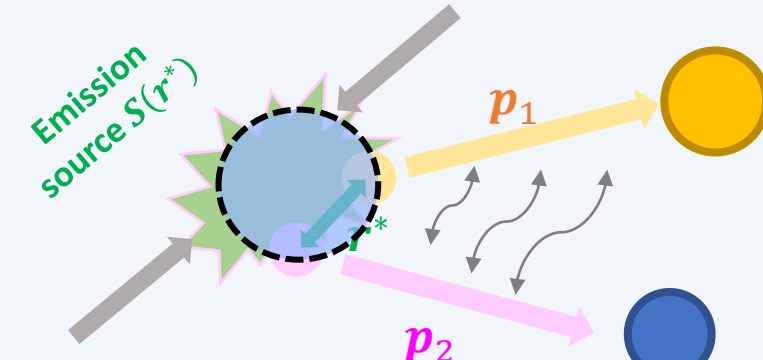
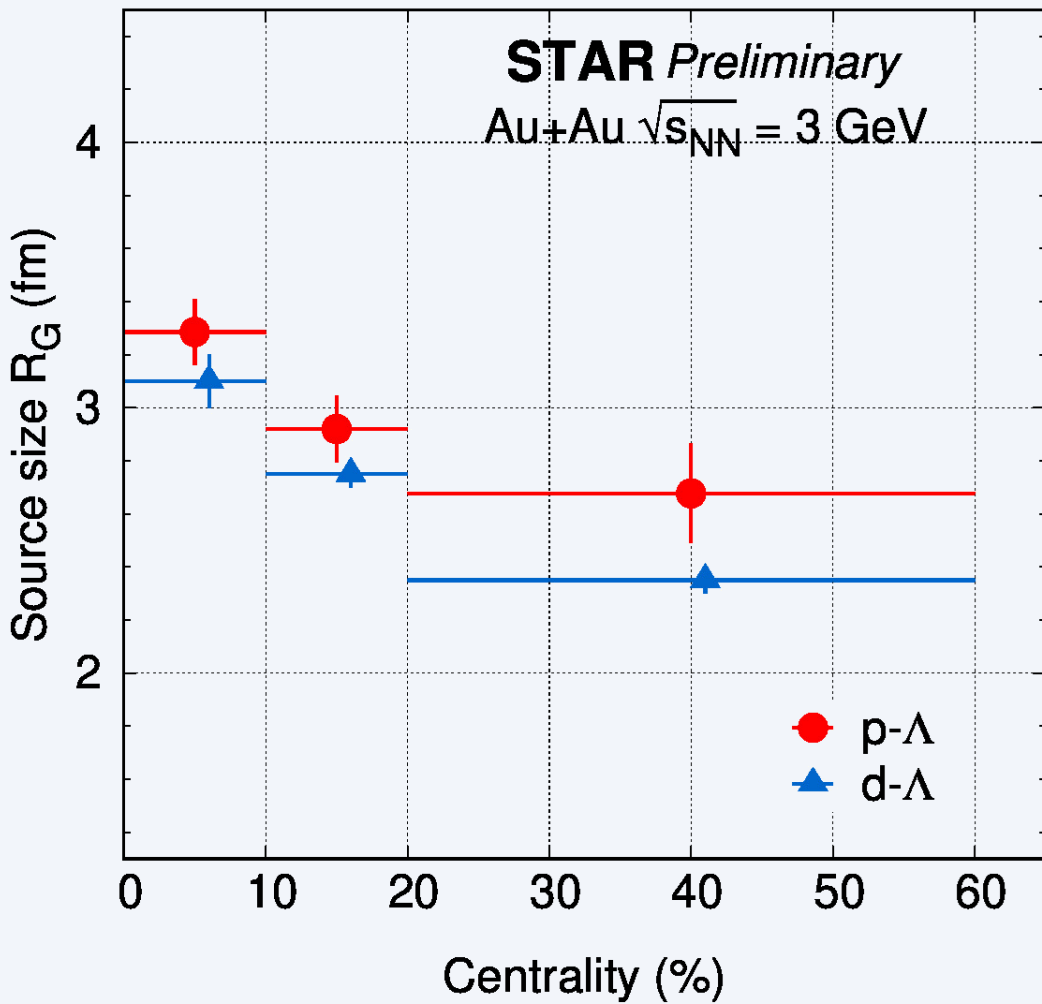
$$\boxed{d_0(Q)}$$

R. Lednický, et al. Sov.J.Nucl.Phys. 35 (1982) 770

L. Michael, et al. Ann.Rev.Nucl.Part.Sci. 55 (2005) 357-402

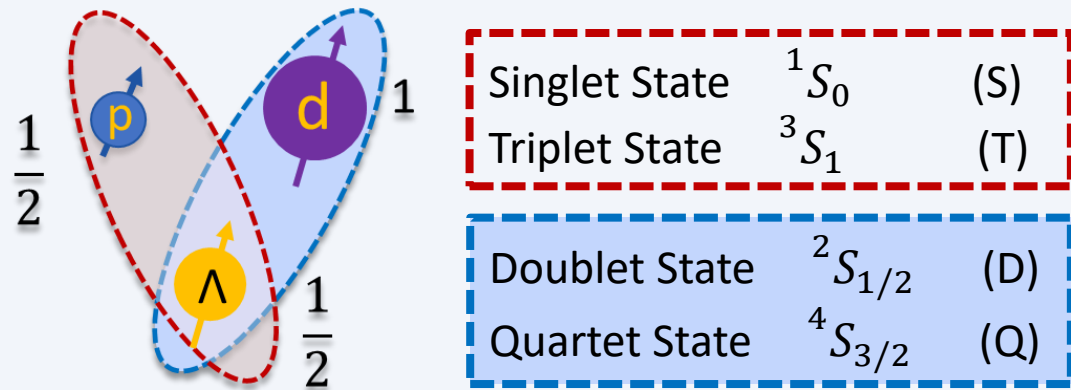
J. Haidenbauer, Phys.Rev.C 102 (2020) 3, 034001

# Source Size with L-L approach



- ❖  $R_G$ : **spherical Gaussian source of pairs** by Lednicky-Lyuboshits approach
- ❖ Separation of emission source from final state interaction
- ❖ Collision dynamics as expected:
  - ❖  $R_G^{\text{central}} > R_G^{\text{peripheral}}$
  - ❖  $R_G(p - \Lambda) > R_G(d - \Lambda)$

# Correlation Function & Spin States



**d-Λ:**  $|\psi(r, k)|^2 \rightarrow \frac{1}{3}|\psi_{1/2}(r, k)|^2 + \frac{2}{3}|\psi_{3/2}(r, k)|^2$

- Different spin states with different  $f_0$  and  $d_0$  parameters
- p-Λ correlation:** current statistics is not enough to separate two spin states → **spin-averaged fit**
- d-Λ correlation:** very different  $f_0$  for (D) and (Q) are predicted → **Spin-separated fit**

